Electronic Supplementary Information

Integrating redox flow battery into Z-Scheme water splitting system for enhancing solar energy conversion efficiency

Zhen Li,[†ab] Wangyin Wang,[†a] Shichao Liao,[a] Mingyao Liu,[ac] Yu Qi,[a] Chunmei Ding[a] and Can Li*[a]

[a] State Key Laboratory of Catalysis, Dalian Institute of Chemical Physics, Chinese Academy of Sciences; Dalian National Laboratory for Clean Energy, Collaborative Innovation Center of Chemistry for Energy Materials (iChEM), Dalian, 116023, China. E-mail: canli@dicp.ac.cn

[b] University of Chinese Academy of Sciences, Beijing 100049, China

[c] Key Laboratory on Fuel Cell Technology of Guangdong Province, School of Chemistry and Chemical Engineering, South China University of Technology, Guangzhou, 510641, China

[†] These authors contribute equally to this work.

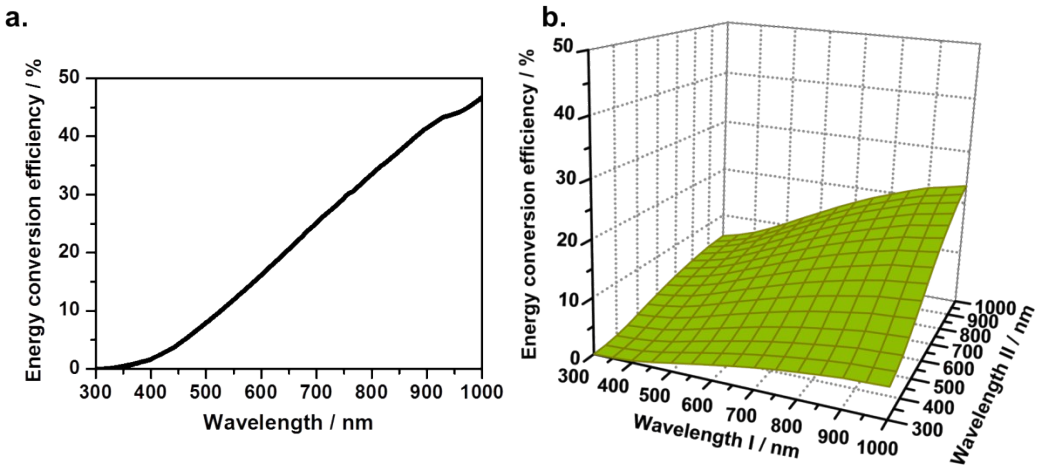

Fig. S1 Theoretical maximal solar energy conversion efficiency as a function of band edge absorption wavelength in one-step water splitting system **a)** and as a function of band edge absorption wavelengths of two semiconductors in Z-scheme water splitting system **b)**. Solar irradiance used for the calculation is taken from AM 1.5G data.

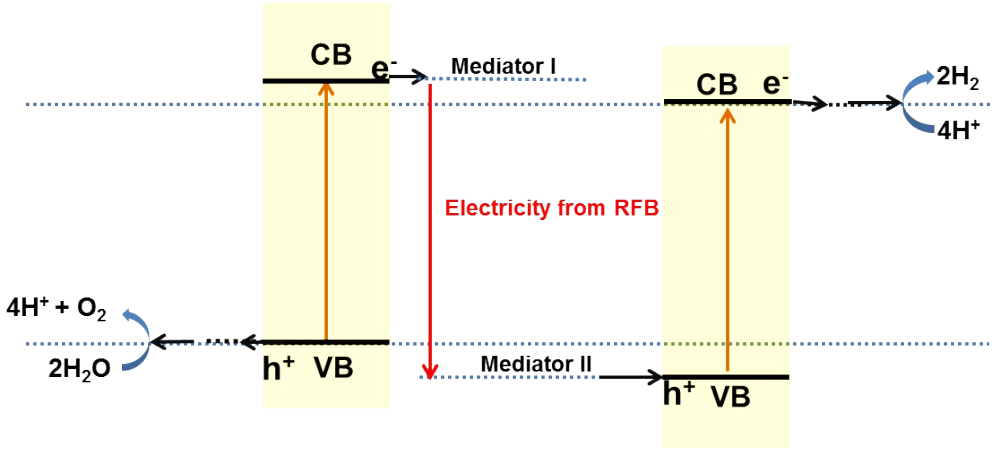

Fig. S2 Schematic of the RFB-integrated Z-scheme water splitting system in an ideal case with the energy efficiency reaching 100%.

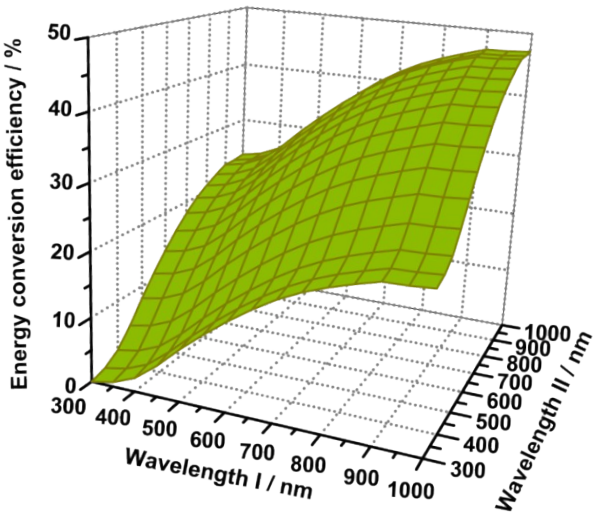

Fig. S3 Theoretical maximal solar energy conversion efficiency as a function of the band edge absorption wavelengths of two semiconductors in the RFB-integrated Z-scheme water splitting system. Solar irradiance used for the calculation is taken from AM 1.5G data.

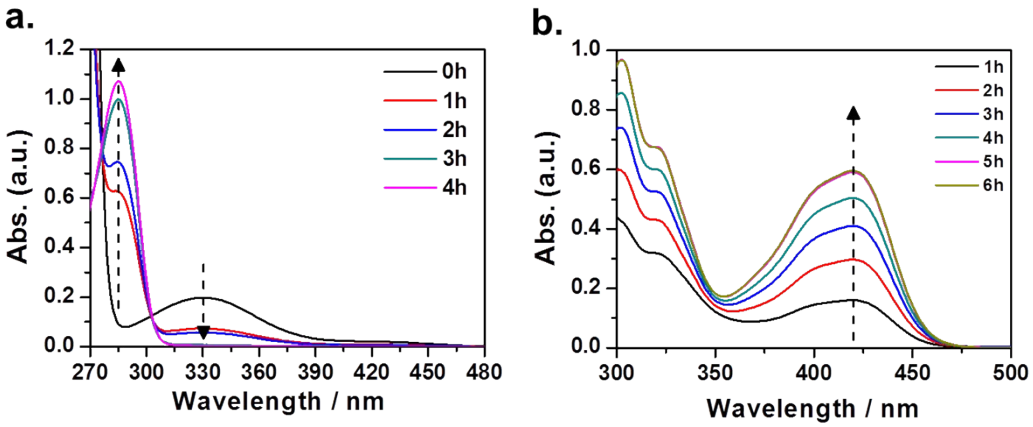

Fig. S4 a) UV-Vis absorption of the 10-times-diluted DMBQ/$DMBQH_2$ solution during the OER-charge process; the increasing absorption centered at 285 nm and the decreasing absorption at 330 nm indicate the conversion from DMBQ to $DMBQH_2$. **b)** UV-Vis absorption of the 20-times-diluted $Fe(CN)_6^{4-}$/$Fe(CN)_6^{3-}$ solution during the HER-charge process; the increasing absorption centered at 420 nm indicates the conversion from $Fe(CN)_6^{4-}$ to $Fe(CN)_6^{3-}$.

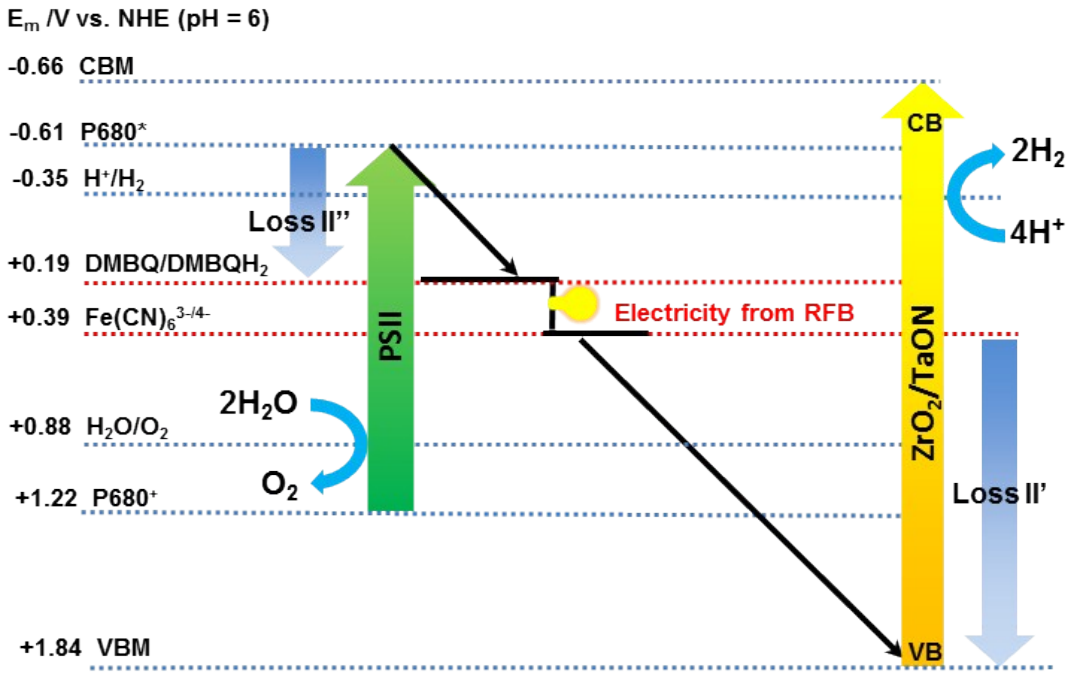

Fig. S5 Schematic of the energy loss and electricity production in the quinone/ferricyanide RFB integrated PSII-ZrO_2/TaON Z-scheme water splitting system.

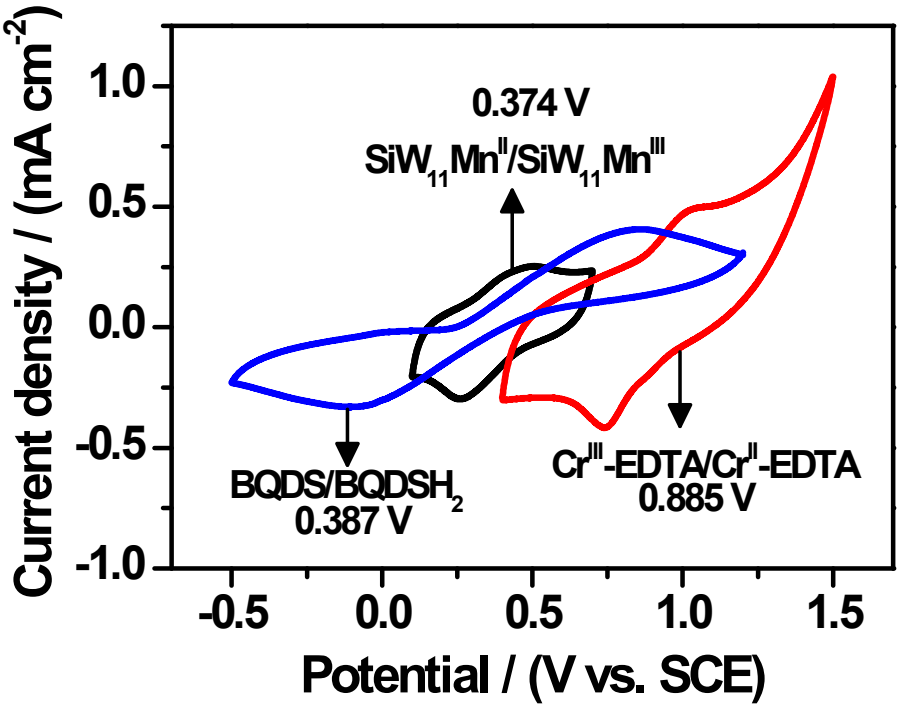

Fig. S6 Cyclic voltammogram curves of 1 mM $BQDSH_2$, $[SiW_{11}O_{39}Mn^{II}(H_2O)]^{6-}$, Cr^{II}-EDTA in 100 mM PBS solution scanned at 50 mV s^{-1}. Cyclic voltammetry tests were performed in a three-electrode system with a graphite plate as the working electrode, a Pt plate as the counter electrode and a saturated calomel electrode as the reference electrode.

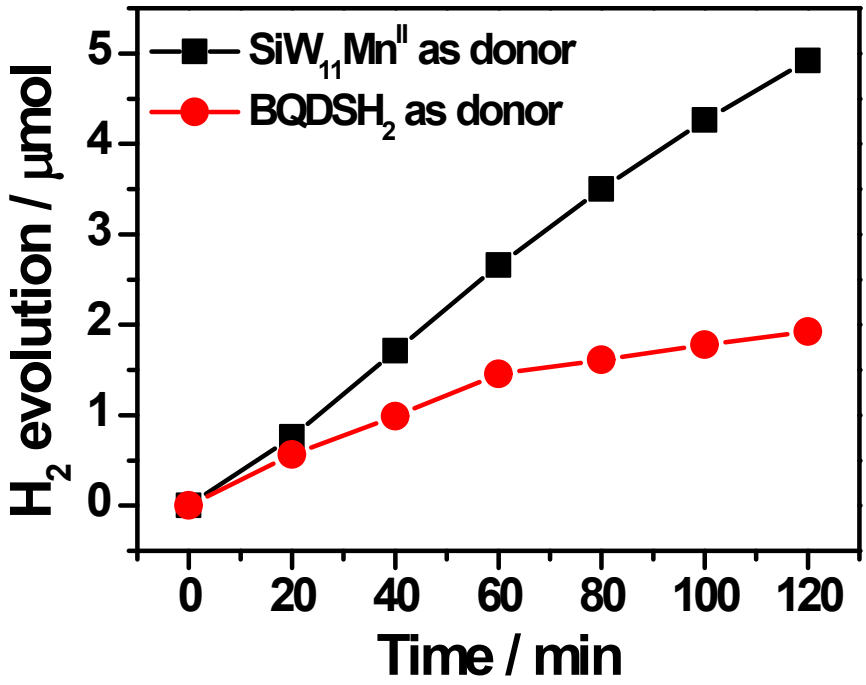

Fig. S7 Time courses of hydrogen evolution by $PtCrO_x$-ZrO_2/TaON with 2.5 mM $[SiW_{11}O_{39}Mn^{II}(H_2O)]^{6-}$ and 10 mM $BQDSH_2$ as electron donors in 20 mL PBS buffer solution. Xenon lamp equipped with a 420 nm long-pass filter was used as light source. Temperature was 25 ℃.